NASA TECHNICAL NOTE

NASA TN D-6767

c. 1

NASA TN D-6767

LOAN COPY: RETURN
AFWL (DOUL)
KIRTLAND AFB, N. M

TECH LIBRARY KAFB, NM

0133601

PARAMETRIC ANALYSIS OF PERFORMANCE AND DESIGN CHARACTERISTICS FOR ADVANCED EARTH-TO-ORBIT SHUTTLES

by Edward A. Willis, Jr., William C. Strack, and John A. Padrutt

Lewis Research Center
Cleveland, Ohio 44135

NATIONAL AERONAUTICS AND SPACE ADMINISTRATION • WASHINGTON, D. C. • APRIL 1972

TECH LIBRARY KAFB, NM

0133601

1. Report No. NASA TN D-6767	2. Government Accession No.	3. Recipient's Catalog No.
4. Title and Subtitle PARAMETRIC ANALYSIS OF PERFORMANCE AND DESIGN CHARACTERISTICS FOR ADVANCED EARTH-TO-ORBIT SHUTTLES		5. Report Date April 1972
		6. Performing Organization Code
7. Author(s) Edward A. Willis, Jr.; William C. Strack; and John A. Padrutt		8. Performing Organization Report No. E-6749
		10. Work Unit No. 110-06
9. Performing Organization Name and Address Lewis Research Center National Aeronautics and Space Administration Cleveland, Ohio 44135		11. Contract or Grant No.
		13. Type of Report and Period Covered Technical Note
12. Sponsoring Agency Name and Address National Aeronautics and Space Administration Washington, D.C. 20546		14. Sponsoring Agency Code

15. Supplementary Notes

16. Abstract

Performance, trajectory, and design characteristics are presented for (1) a single-stage shuttle with a single advanced rocket engine, (2) a single-stage shuttle with an initial parallel chemical-engine and advanced-engine burn followed by an advanced-engine sustainer burn (parallel-burn configuration), (3) a single-stage shuttle with an initial chemical-engine burn followed by an advanced-engine burn (tandem-burn configuration), and (4) a two-stage shuttle with a chemical-propulsion booster stage and an advanced-propulsion upper stage. The ascent trajectory profile includes a brief initial vertical rise; zero-lift flight through the sensible atmosphere; variational steering into an 83-kilometer-by-185-kilometer intermediate orbit; and a fixed, 460-meter per-second allowance for subsequent maneuvers. Results are given in terms of burnout mass fractions (including structure and payload but not the engine), trajectory profiles, propellant loadings, burn times, etc. These results are generated with a trajectory analysis that includes a parametric variation of the specific impulse from 800 to 3000 seconds and the specific engine weight from 0 to 1.0.

17. Key Words (Suggested by Author(s)) Nuclear space shuttle; space shuttle; shuttle; Launch vehicle(s); Nuclear launch vehicle(s); Nuclear propulsion	18. Distribution Statement Unclassified - unlimited

19. Security Classif. (of this report)	20. Security Classif. (of this page)	21. No. of Pages	22. Price*
Unclassified	Unclassified	31	$3.00

* For sale by the National Technical Information Service, Springfield, Virginia 22151

PARAMETRIC ANALYSIS OF PERFORMANCE AND DESIGN CHARACTERISTICS FOR ADVANCED EARTH-TO-ORBIT SHUTTLES

by Edward A. Willis, Jr.; William C. Strack; and John A. Padrutt

Lewis Research Center

SUMMARY

A parametric study of earth-to-orbit shuttles using hypothetical advanced rocket engines covered the following conditions: specific impulse of the advanced engine, 800 to 3000 seconds; specific engine weight, 0 to 1.0; vehicle configurations, (1) single-stage vehicle with an advanced engine only, (2) single-stage vehicle with parallel-burning hybrid (chemical plus advanced) propulsion, (3) single-stage vehicle with tandem-burning hybrid (chemical followed by advanced) propulsion, and (4) two-stage vehicle with chemical-propulsion booster and an advanced-propulsion upper stage. The ascent trajectory profile includes a brief initial vertical rise; zero-lift flight through the sensible atmosphere; variational steering into an 83-kilometer-by-185-kilometer intermediate orbit; and a fixed, 460-meter-per-second allowance for subsequent maneuvers. Performance, expressed as the sum total of payload, structure, and radiation shielding fractions delivered to orbit, is maximized through the use of the variational steering program and by optimizing the advanced-engine sizes.

The results are intended as an aid in rapidly evaluating the usefulness of advanced engine concepts for launch propulsion. Once the thrust, weight, and specific impulse characteristics have been determined for a class of engines, the appropriate engine size, burn time or times, stage mass fraction or fractions, and other design information can be read directly from the present results. Payload ratios can also be determined by combining the present results with the user's estimate of structure and radiation shielding fractions for a particular system. Alternatively, vehicle design goals in the structure and shielding areas can be rationally chosen in terms of known engine characteristics. Finally, lower-bound structure estimates may be applied to the present results to identify concepts that do not make sense in terms of an earth-to-orbit launch mission. For example, a structural ideal weight fraction of about 0.25, derived from recent chemical-propulsion space shuttle studies, is surely a lower bound for functionally equivalent nuclear stages (which would be penalized by lower average fuel densities and by the need for radiation shielding). On this basis, it may be concluded that advanced nuclear engines in the 1800- to 3000-second range must have specific weights lower than 0.25 to 0.40, respectively, if they are to be considered for launch vehicle application.

INTRODUCTION

Launch costs have been an item of major concern since the earliest days of the space program. Although many cost-reduction principles might be applied to conventional launch vehicles, they will yield only incremental improvements in cost effectiveness as long as the launch vehicle is discarded after each use. A fully reusable system is needed to reduce launch costs to really attractive levels, for example, below $400 per kilogram in orbit. Therefore, the so-called "space shuttle" is under intensive study.

According to one concept, the shuttle could consist of two airplane-like stages with chemical oxygen-hydrogen rockets for primary propulsion. Each stage would independently reenter the atmosphere and fly back to base on turbofan power, after supplying its assigned velocity increment. Unfortunately, the large deadweight fractions associated with reentry structure lead to poor payload ratios, even for a two-stage vehicle. Thus, while this shuttle concept may eventually offer low operating costs because of being completely reusable, it is almost certain to be extremely large in comparison to its payload and to involve a very large initial investment. In addition, the use of two stages introduces complexities (and presumably costs) into the design, testing, and operational programs that would not be present with an otherwise similar single-stage design.

In the hope of avoiding these disadvantages, the present report considers the use of advanced, high-specific-impulse engines as an integral part of the earth-to-orbit propulsion. The term "advanced" is used here and throughout this report to connote the class of propulsion concepts having specific impulses considerably higher than present chemical rockets. The class thus includes, but is not necessarily limited to, the various forms of nuclear rockets. Some performance estimates for nuclear rockets have been given in the past, for example, those reported in reference 1. These however apply only to the particular engine studies and, in many cases, were of a very approximate nature (e.g., neglecting drag, gravity, or both). Considering the potential long-range consequences of an incorrect determination, there is a need for general results that can quickly provide accurate and consistent performance comparisons between diverse kinds of advanced engines.

Accordingly, the present report states the results of a wide range of accurate earth-to-low-orbit launch trajectory simulations. These are based on a realistic model of the earth's gravity field and atmosphere, representative launch vehicle aerodynamic characteristics, and typical velocity increment ΔV reserve allowances for postinjection maneuvers. Four combinations of engine, vehicle, and trajectory are studied, as shown in figure 1:

(1) A single stage to orbit using a single advanced engine (fig. 1(a)).

(2) A single stage to orbit with chemical and advanced propulsion in the boost phase but only advanced propulsion in the sustainer phase. The chemical engines are shut down at the optimum propulsion transition altitude (fig. 1(b)).

(3) A single stage to orbit using only chemical propulsion during the boost phase and only advanced propulsion in the sustainer phase. The propulsion transition altitude is constrained to be above the earth's sensible atmosphere (fig. 1(c)).

(4) Two stages to orbit using a chemical booster stage followed by an advanced upper stage (fig. 1(d)). The staging altitude is constrained as in case 3.

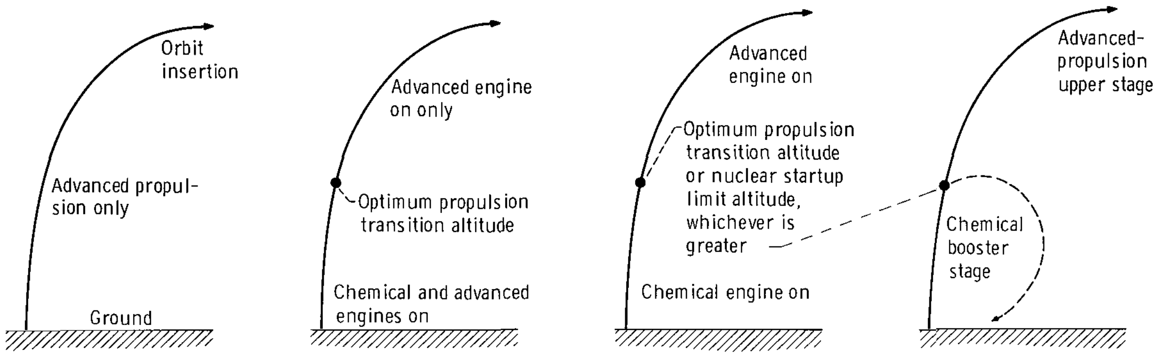

(a) Single stage with all advanced propulsion.

(b) Single stage - parallel burn (chemical augmentation during boost phase).

(c) Single stage - tandem burn (chemical boost phase followed by advanced-propulsion upper stage).

(d) Two stage (chemical booster and advanced-propulsion upper stage).

Figure 1. - Vehicle trajectory configurations.

The first two vehicle/trajectory combinations were designed to take maximum advantage of the advanced engine's performance potential. The second two, although generally applicable, were designed primarily for the benefit of nuclear engines (for which the ground-start feature may be unacceptable).

Hypothetical advanced engines are considered which range from 800 to 3000 seconds in vacuum specific impulse and from 0 to 1.0 in specific weight (engine weight/vacuum thrust ratio). The ascent trajectory profile includes a brief initial vertical rise; zero-lift flight through the sensible atmosphere; variational steering into an 83-kilometer-by-185-kilometer intermediate orbit; and a fixed, 460-meter-per-second allowance for subsequent maneuvers. Maximum performance is ensured by using variational steering above the sensible atmosphere and by optimizing the size of the advanced engine. For cases 2, 3, and 4, the chemical booster engines are sized to produce a ratio of sea-level thrust to initial gross weight of 1.2.

There are obvious difficulties in estimating the proper structural and radiation shield weight fractions for unknown vehicles combined with parametrically defined engines. Hence, the present results are presented in terms of burnout weight in final orbit, excluding the advanced engine. That is, payload, structure, and shielding (if any) are lumped together and expressed as a fraction of the initial gross weight.

SYMBOLS

A	vehicle reference area, m^2
A_e	engine (nozzle) exit area, m^2
a_o	ratio of stage vacuum thrust to vehicle gross initial weight
C_D	vehicle drag coefficient
F	thrust, N
I	specific impulse, sec
P	atmospheric pressure, N/m^2
q	dynamic pressure, N/m^2
R	ratio of stage burnout weight to vehicle gross initial weight
w_{fs}	thrust-sensitive weight fraction, i.e., engine specific weight
w_p	ratio of stage propellant weight to vehicle gross initial weight
w_{pay}	ratio of payload weight in orbit to vehicle initial gross weight
w_{ps}	propellant-sensitive deadweight fraction
α	initial kick angle (relative to local horizontal), deg
θ	pad-to-vehicle look angle, deg
ψ	thrust angle (relative to local horizontal), deg
$\dot{\psi}$	thrust angle pitch rate, deg/sec

Subscripts:

C	chemical
N	nuclear, or advanced
v	vacuum

CHARACTERISTICS OF PROSPECTIVE ADVANCED ENGINE CONCEPTS

In order to associate these parametric variables with physical systems, it is appropriate to briefly review the performance and operating characteristics anticipated for several advanced engine concepts that might be considered for launch vehicle propulsion.

Solid-Core Nuclear Rocket

The solid-core nuclear rocket (SCNR) is the only one of the engines to be discussed that could be brought to operational status within this decade. It operates on a simple principle: the heating of hydrogen to produce thrust. In the present case the heating is done by a reactor constructed of solid fuel elements and structure. To keep these parts from melting, the reactor temperature, and hence the hydrogen temperature, is limited to values less than 3300 K. Correspondingly, the maximum specific impulse attainable by this concept is only a little greater than 900 seconds. The NERVA program has already demonstrated that a value of at least 800 seconds can be attained in practice.

Despite optimistic early estimates, such engines are more than an order of magnitude heavier than chemical engines of comparable thrust. NERVA-class, SCNR specific weights (engine weight/vacuum thrust) are now in the range of approximately 0.3 to 0.4. At these levels, SCNR upper stages show only minor performance gains for earth-to-orbit launch propulsion (refs. 2 and 3).

Moreover, the SCNR by its nature retains a sizable inventory of radioactive fission fragments and therefore creates a severe postfiring radiation hazard. Even if other problems are neglected, it is difficult to see how this one characteristic of the SCNR could be reconciled with the manned, recoverable, rapid-turnaround style of operation envisioned for the shuttle. Perhaps for these reasons, recent SCNR application studies, such as reference 4, consider only high-orbit, lunar, or interplanetary missions with orbital startup.

On the other hand, advanced engine research continues, and several encouraging trends may be observed. For example, the present NERVA engine, with continuing support, could most likely be considerably upgraded through evolutionary improvements - primarily, higher temperature fuel elements and more efficient shielding. Furthermore, several nonadvanced propulsion concepts are now under study; one or more of these may offer a revolutionary advance in the more distant future.

Fluidized Dust-Bed and Liquid-Core Rockets

Fluidized dust-bed (FDB) and liquid-core (LC) rockets are similar to the SCNR in that the fuel material heats hydrogen to produce thrust. In the FDB, however, the fuel is a finely divided powder or dust and is held by centrifugal force against the periphery of a rotating drum. Inwardly flowing hydrogen penetrates and fluidizes the dust bed and then turns and flows axially into the nozzle. The LC is similar except that the fuel is actually molten. Their common advantage is that a higher reactor exit hydrogen temperature can be achieved, since the fuel material itself is at a higher temperature. Studies such as reference 5 indicate that a specific impulse of 930 to 1000 seconds, and a specific weight of 0. 1 to 0. 2 may be achievable by the FDB concept. The LC engine gives somewhat higher impulse but is considerably heavier.

The in-flight radiation characteristics of these engines would presumably be similar to those of the SCNR. At shutdown, however, it is possible in principle to discharge the fuel material through the nozzle, thus avoiding (or at least, relocating) the postfiring radiation hazard.

Gas-Core Nuclear Rocket

Another way to avoid temperature limitations is to have the fuel in the form of an extremely hot fissioning plasma ball which heats hydrogen primarily by radiation. This is called the gas-core nuclear rocket (GCNR). The plasma is separated from the hydrogen, either approximately, by hydrodynamic means, in the so-called "open cycle" engine; or completely, by means of a transparent mechanical barrier, in the closed-cycle (or "light bulb") engine. In either case, a small amount of "seed" material (e.g., tungsten or depleted uranium powder) is added to improve the hydrogen's radiative absorption properties.

In this area, basic research has resulted in apparent progress toward a demonstration of feasibility. Laboratory tests applicable to the open-cycle concept (ref. 6) indicate that the necessary types of flow pattern, uranium plasma confinement, separation, etc., can be achieved under conditions suggestive of a GCNR reactor. Engine specific weights as low as 0. 50 to 0. 33 and specific impulse in the 1500- to 3000-second range are predicted by that study (see ref. 7) and yield good performance for interplanetary missions (ref. 8). Aside from radiation-safety concerns it would also appear promising for earth launch missions. It would not present a major radiation hazard after shutdown since the fission fragment inventory is not retained. It does, however, discharge a small amount of partly fissioned uranium and/or activated seed material (e.g., 1 percent of the hydrogen flow rate) at all times during operation, and this is evidently an undesirable feature from the atmospheric pollution viewpoint if a low-altitude startup is envisioned. On the other hand, the closed-cycle, or light bulb, engine (ref. 9) may discharge very little radioactive debris and hence would be less subject to this objection.

Nuclear Pulse Rockets

In the original nuclear pulse rocket (NPR) concept, part of the momentum/energy flux from a series of nuclear bomb explosions would be intercepted by a shock-absorbing "pusher plate" mechanism, which in turn would impart forward velocity impulses to the space vehicle. Early studies indicated average specific impulses and specific weights in the range of possible interest for launch vehicle applications. From a strictly technical viewpoint, this may well be the most nearly practical of the presently known advanced nuclear propulsion concepts beyond the SCNR. Alone among the "advanced" devices mentioned herein, its fundamental physical mechanism - the explosion of nuclear bombs - is definitely known to be feasible. It has an added advantage in that its "fuel" is extremely dense, and thus lends itself to a compact, lightweight structural design.

On the other hand, this is inherently a "dirty" propulsion device. Some recent research has therefore been directed toward the "mini-bomb" approach which uses fusion (rather than fission) explosions. These can be made essentially "clean" because the fusion reaction is initiated by a separate mechanism, such as a relativistic electron beam, rather than by a fission explosion. No weight estimates are available for this type of engine at present.

Beamed-Energy Rockets

A distinctly different concept, beamed-energy rockets (BER), makes use of ground-generated electrical power which is beamed to the launch vehicle by very intense laser or microwave beams. The beamed energy is used on board the vehicle to heat a working fluid, which is then expelled to produce thrust. There is no radiation hazard because no nuclear processes occur on board the vehicle. One form of this concept has been studied briefly in reference 10. Although very preliminary in nature, the results indicate that a specific impulse of several thousand seconds and a specific weight comparable to that of present chemical engines may be attainable.

ANALYSIS

As explained in the INTRODUCTION section, the present results are primarily developed in terms of total burnout weight fractions, excluding the advanced engine. These may be combined with vehicle configuration, structure, and shielding studies (not included herein) to arrive at final payload ratios or other parameters of interest.

Vehicle Mass

In the following equations the payload weight w_{pay}, the residual burnout weight R, the engine thrust a_o, and the propellant weight w_p are all expressed as fractions of the gross initial weight of the entire vehicle. The engine specific weight w_{fs} is expressed as a fraction of vacuum thrust and includes thrust-sensitive structure and installation details. Structural weight w_{ps} is given in terms of propellant weight.

By using propellant mass ratios determined from trajectory simulation (to be discussed in the next section) along with the chosen engine thrust levels, engine specific weight, and assumed tank structure fraction, the final payload ratio may be written simply as

$$w_{pay} = R_N - a_{o,N}w_{fs,N} - w_{p,N}w_{ps,N} \tag{1a}$$

for the single-stage, all-advanced-propulsion case (fig. 1(a)). The same equation applies to the upper stage of the two-stage case (fig. 1(d)) after allowing for the fact that a booster stage has been jettisoned. The relation

$$w_{pay} = R_N - a_{o,N}w_{fs,N} - w_{p,N}w_{ps,N} - a_{o,C}w_{fs,C} - w_{p,C}w_{ps,C} \tag{1b}$$

applies for the two hybrid-propulsion, single-stage cases (figs. 1(b) and (c)).

As previously mentioned, the payload and structure weights are lumped together for the purposes of this study. The quantities to be actually presented are given by

$$w_{pay} + w_{p,N}w_{ps,N} = R_N - a_{o,N}w_{fs,N}$$

and

$$w_{pay} + w_{p,N}w_{ps,N} + w_{p,C}w_{ps,C} = R_N - a_{o,N}w_{fs,N} - a_{o,C}w_{fs,C}$$

which follow from equations (1a) and (1b), respectively.

For two-stage vehicles the values entering equation (1a) allow for the fact that an optimally sized booster stage has been previously jettisoned. For this case only, it is necessary to assume definite values for the chemical- and nuclear-stage structure fractions ($w_{ps,C}$ and $w_{ps,N}$) because, as explained in reference 11, they enter into the variational transversality condition that defines the optimum staging point. Values of 0.22 and 0.27 were assumed for $w_{ps,C}$ and $w_{ps,N}$, respectively); these values are similar to those suggested in early shuttle studies.

Trajectory Calculations

Each trajectory was calculated by using the numerical integration computer program described in reference 11. This program maximizes the payload of a multistage launch vehicle by finding the best propellant loadings and best thrust steering control outside the sensible atmosphere. (The trajectory simulation to be discussed here applies only to this study and does not describe the general capabilities of the ref. 11 computer program.) As illustrated in figure 2, the trajectory simulation consists of a short vertical

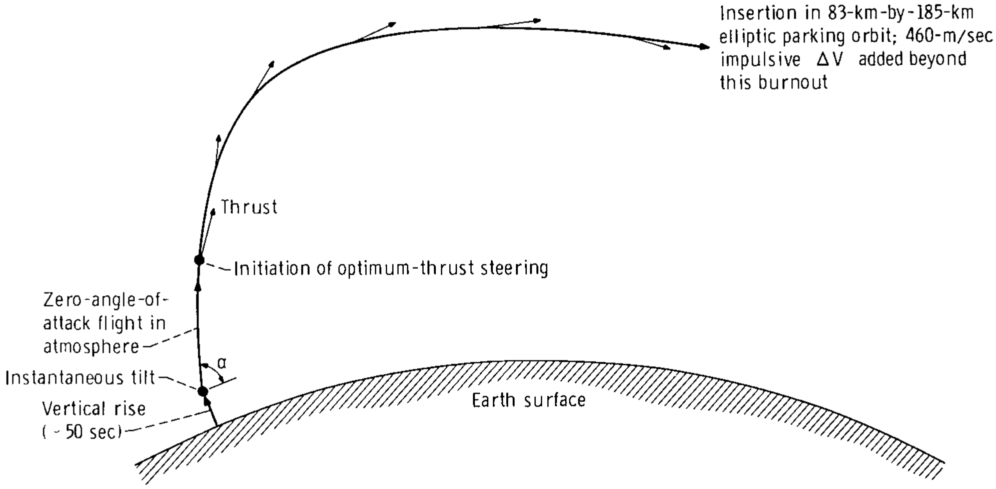

Figure 2. - Trajectory profile in launch azimuth plane.

rise from Cape Kennedy, of fixed duration, after which the vehicle is tilted over instantaneously at some small angle α in the 90° azimuth direction. The angle α is optimized for the trajectory. The thrust vector is then constrained to the launch azimuth plane with zero angle of attack in the pitch plane until aerodynamic loads and heating are negligible. During this portion of the trajectory, aerodynamic and oblate rotating earth effects are included.

This portion is terminated either when the vehicle reaches 30 kilometers altitude (assumed to be the limit of the sensible atmosphere) or when a propulsion transition takes place, whichever occurs last. Following this portion, a planar optimum-thrust portion is initiated that ignores aerodynamic and oblateness effects (presumably negligible by this time) and uses the optimum-thrust steering control determined by the calculus of variations. To be perfectly consistent, it would have been preferable to always start the optimum-thrust steering program at 30 kilometers. However, this requires considerably more labor since the computer program has no provision for altitude-dependent phase changes. Hence, the results in some cases are somewhat conservative due to a late shift to unconstrained optimal steering. Payload errors due to this effect are quite small, though, and are insignificant for a study of this nature. This optimum-thrust burn continues until the vehicle attains an 83-kilometer-by-185-kilometer elliptical orbit at the optimum true anomaly (always near perigee). A 460-meter-per-second impulsive ΔV capability above the low earth orbit is added to simulate a space station rendezvous at 480 kilometers altitude, deorbiting, and reserves. Use of the intermediate elliptic orbit is a carryover from previous chemical rocket shuttle studies and is not necessarily desirable for the vehicles of the present analysis. However, limited calculations for more optimal trajectories provided only negligible improvements in vehicle payload capability. On the other hand, the reader is cautioned that variables such as the trajectory shape and peak altitude that are strongly dependent on this assumption could differ appreciably under another ground rule.

For multistage vehicles, the stage burn times may be left open for optimization. This was done for the fourth mission option (chemical first stage, advanced second stage) and significantly increased the difficulty in obtaining converged trajectories due to the high sensitivity of the final conditions to first-stage burn time.

During the zero-angle-of-attack portion the thrust is defined by

$$F = F_V - A_e P$$

where F is the thrust, F_V is the vacuum thrust, A_e is the engine exit area, and P is the atmospheric pressure. The drag is calculated from the equation

$$\text{Drag} = C_D q A$$

where C_D is the drag coefficient, q is the dynamic pressure, and A is the reference area. The drag coefficient curve used in the calculation (fig. 3) is representative of current launch vehicles. A realistic drag curve for an advanced-propulsion shuttle might differ substantially from this curve, but the results presented herein would not be affected significantly by such a change. The reference area A is assumed to be 10^{-4} square meter per kilogram of vehicle gross mass, and nozzle exit area A_e is assumed to be 0.91×10^{-6} square meter per newton of vacuum thrust. These are estimates for a hydrogen-fueled nuclear shuttle. During the optimum-thrust portion, drag is ignored and $F = F_V$.

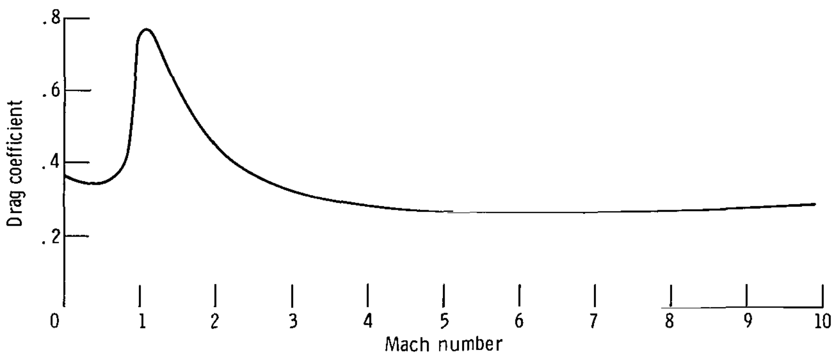

Figure 3. - Assumed drag coefficient curve.

The initial thrust-to-weight ratio was optimized for the all-advanced-propulsion configuration. For the other configurations the launch thrust-to-weight ratio was fixed at 1.2 since chemical-propulsion performance is not sensitive to this variable. The chemical-engine vacuum specific impulse is assumed to be 440 seconds. Other implied assumptions include the instantaneous change in angle of attack at the beginning of the optimum-thrust steering portion and the instantaneous startup and shutdown of full thrust. None of these assumptions should cause a substantial error in the type of results sought in this study.

RESULTS AND DISCUSSION

Three categories of results are included here: (1) performance in terms of burnout weight fraction; (2) trajectory characteristics in terms of shape, peak altitude, and propulsion transition altitude; and (3) design characteristics in terms of thrust levels, burn times, and propellant ratios. For the sake of brevity, the trajectory results and design characteristics are presented for 3000 seconds specific impulse only. These are representative, but not exact, for the other values of specific impulse.

Single Stage - Advanced Propulsion

The single-stage, advanced-propulsion configuration (fig. 1(a)) is discussed first because it is the most straightforward of the configurations and because it offers the best performance in many cases.

Performance. - The burnout weight fraction for this case is plotted in figure 4 as a function of specific engine weight and vacuum specific impulse. The burnout weight fraction includes the payload and all deadweight (i.e., structure, airbreathing engines

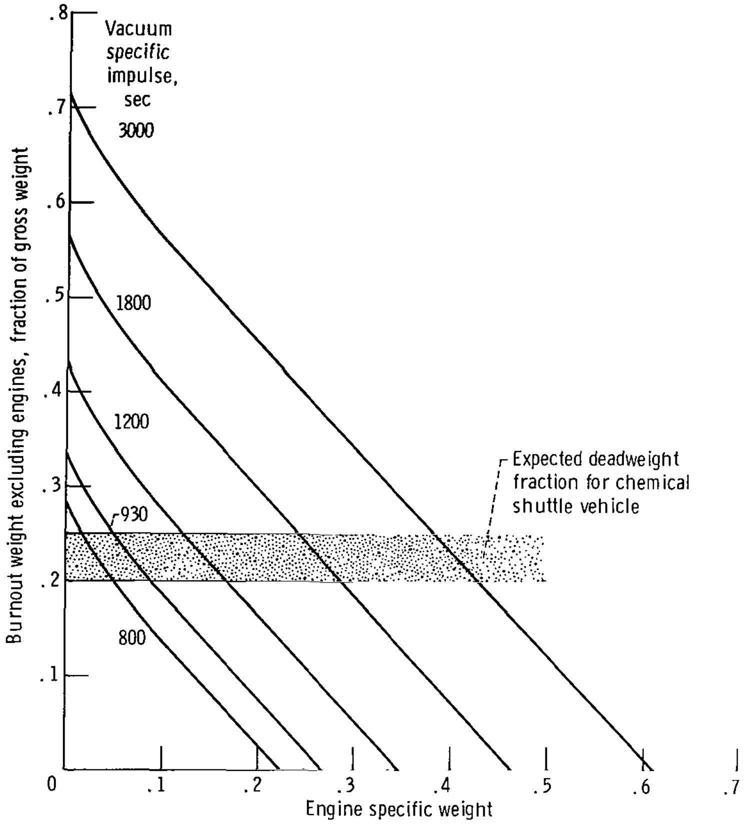

Figure 4. - Performance of single-stage shuttle with all advanced propulsion. Final orbit, 83-kilometer-by-185-kilometer ellipse with 460-meter-per-second additional velocity increment ΔV capability.

with fuel, radiation shielding, and other shuttle equipment) except the advanced engine. Payload capability is determined by subtracting an estimate for the deadweight from the plotted burnout weight. For example, current estimates for a chemical shuttle stage deadweight fraction are about 0.20 to 0.25. Assuming that 0.25 represents a lower limit for a nuclear stage, a single-stage nuclear shuttle with a 930-second vacuum specific impulse engine could not deliver any payload unless the engine specific weight were less than 0.05. A solid-core engine like NERVA having a specific impulse of about 800 seconds could not deliver positive payloads unless the specific engine weight were less than 0.02. Assuming that the specific weight of these engines is roughly 0.30, it can be concluded that current solid-core nuclear rockets are far from being attractive in this application. As another example, suppose that a gas-core nuclear rocket has an 1800-second specific impulse and a vehicle deadweight fraction of 0.25. The allowable engine specific weight for zero payload is 0.24. If the specific weight were really 0.15, the payload fraction would be 0.10 (0.35 - 0.25 = 0.10). Obviously the gas-core nuclear rocket would look attractive under these conditions, but the technology is far from the

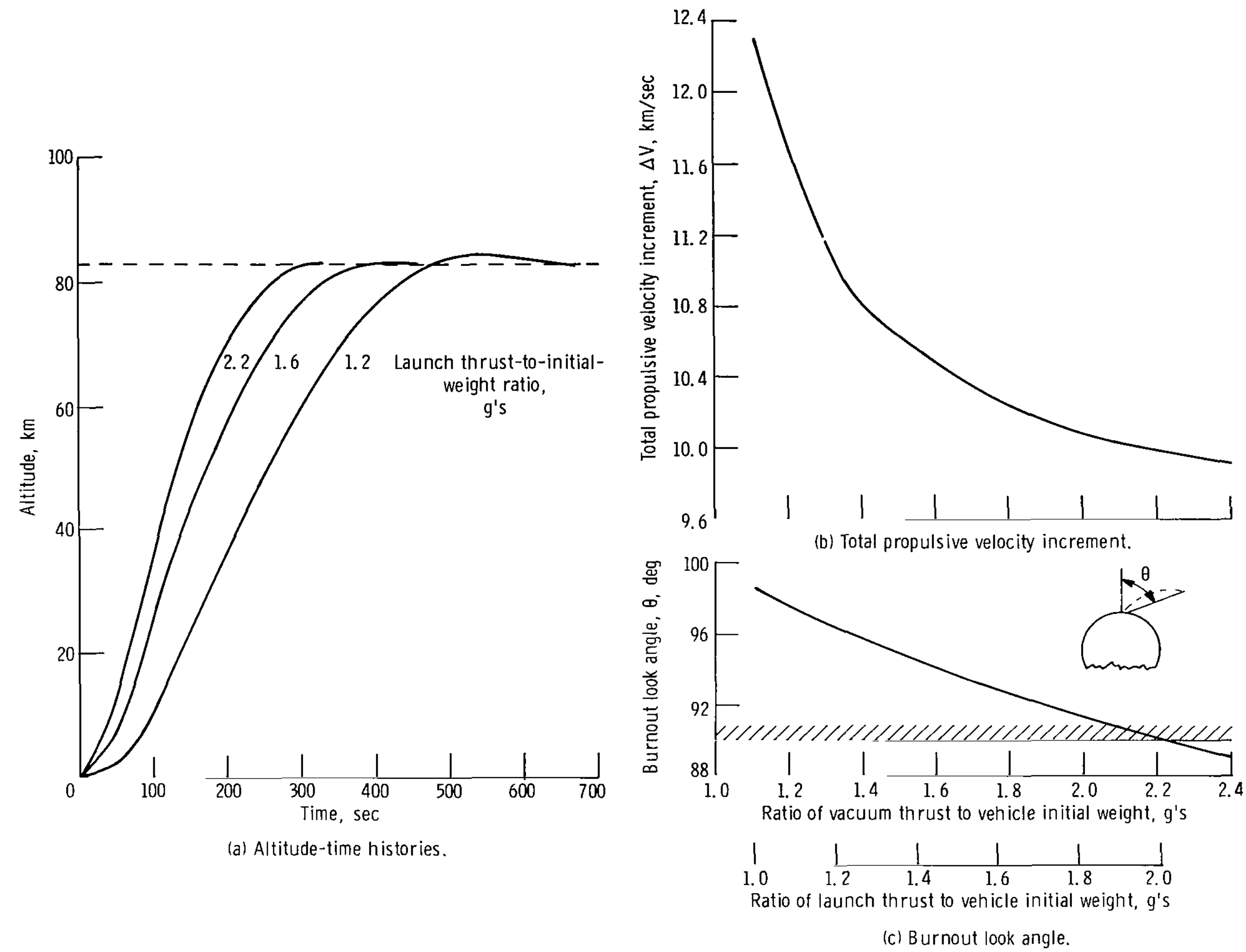

Figure 5. - Trajectory characteristics of single-stage shuttle with all advanced propulsion. Advanced-engine vacuum specific impulse, 3000 seconds; final orbit, 83-kilometer-by-185-kilometer ellipse with 460-meter-per-second additional velocity increment ΔV capability.

construction of even a prototype engine. All that can be said now is that it could not be useful in this application unless its specific engine weight were less than about 0.24.

Trajectory characteristics. - Figure 5(a) displays the trajectory-altitude-against-time histories for the case of 3000-second specific impulse. Curves for several different launch thrust-to-weight ratios are shown. These trajectories are fairly typical of chemical launch vehicle trajectories.

Figure 5(b) shows that the velocity increment ΔV is less than 10 kilometers per second at thrust-to-weight ratios greater than 2. As shown in figure 6(a) the optimum thrust-to-weight ratio is much less than 2 due to the high engine weight.

In some cases it may be desirable to beam ground-computed guidance signals and/or propulsion energy directly from the launch-pad area to the rocket. Such schemes require a continuous line of sight between the launch pad and the vehicle; otherwise, two

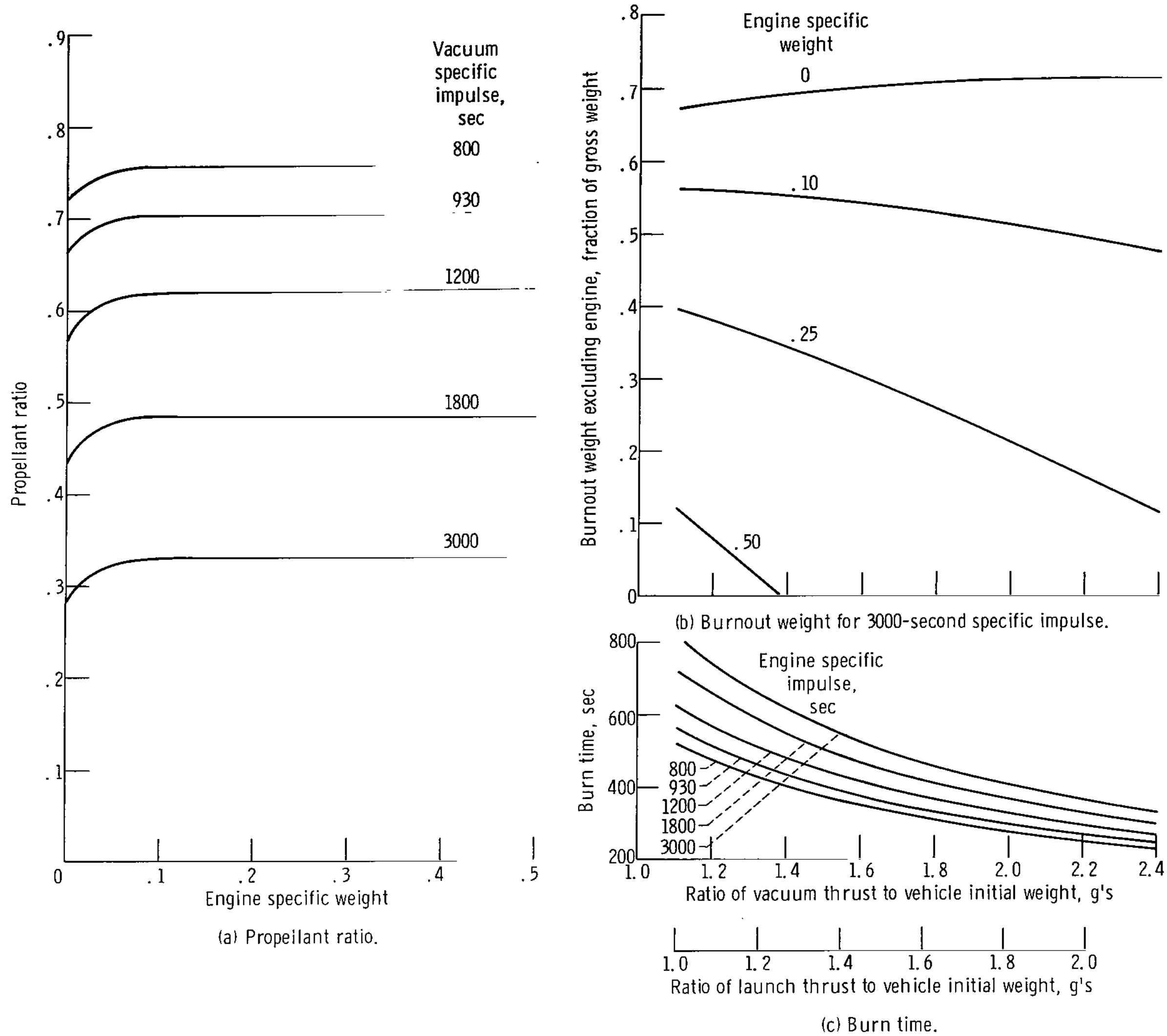

Figure 6. - Design characteristics for single-stage shuttle with all advanced propulsion. Final orbit, 83-kilometer-by-185-kilometer ellipse with 460-meter-per-second additional velocity increment ΔV capability.

or more ground-based installations are required. Specifically, the burnout look angle (defined as the angle between the launch vertical and the pad-to-burnout line) must be less than 90° to avoid multiple transmitter installations. Burnout look angle is plotted against initial thrust-to-weight ratio in figure 5(c). At low values of initial acceleration the burnout look angle exceeds 90°. Thus, for beam-guided or beamed-energy rockets, two transmitter installations are required unless the initial thrust-to-weight ratio is greater than 2 or unless specially shaped, less efficient trajectories are used.

Design characteristics. - The values of several mission-determined variables are of special importance to the hardware designer. Propellant ratio, optimum thrust level, and burn time are examples. Propellant ratio (propellant weight/gross weight) curves are shown in figure 6(a). For 3000 seconds specific impulse the propellant ratio is about 0.33, while for 800 seconds it is about 0.75.

The effect of varying the initial thrust-to-weight ratio on burnout weight is shown in figure 6(b) for a specific impulse of 3000 seconds. For very light engines the optimum initial thrust-to-weight ratio may approach 2; however, the performance penalty is insignificant over a wide range of thrust-to-weight ratios. The optimum initial thrust-to-weight ratio falls rapidly to its lower limit value of 1.0 as the engine specific weight increases; and, at the same time, the performance curves steepen considerably. The performance curves at the other specific impulse values are qualitatively quite similar - in all cases the optimum initial thrust-to-weight ratio is 1.0 for specific engine weights greater than 0.1. Such low lift-off acceleration is clearly undesirable from an operational viewpoint but is necessary to achieve the advanced engine's full performance potential.

The burn time required for this configuration is shown in figure 6(c). Raising the specific impulse or lowering the launch acceleration increases the burn time, but in no case is it greater than 900 seconds.

Single Hybrid Stage - Parallel-Burn Configuration (Parallel Chemical Plus Advanced Initial Burn Followed by Advanced Sustainer Phase)

The poor performance of the all-advanced-propulsion single-stage shuttle at high engine specific weight suggests adding chemical engines for use during the early boost phase. This permits the advanced engine to be smaller and alleviates its high weight penalty. In the parallel configuration both chemical and advanced engines are started on the launch pad, and then the chemical engine is shut down at the optimum time and altitude (fig. 1(b)). The optimum thrust angle program begins either at the propulsion transition altitude or 30 kilometers, whichever is greater. The launch thrust-to-weight ratio is fixed at 1.2 (unless zero chemical propulsion is optimum), and the total thrust is optimally split between advanced and chemical engines for maximum burnout weight.

Performance. - The burnout weight fraction for this mode is shown in figure 7(a). At the low end of the specific weight range the advanced engine's high specific impulse eliminates the chemical propulsion, and the performance curves match the all-advanced-propulsion curves given in figure 4. But at high engine specific weights the performance curves flatten out horizontally toward the all-chemical case of 0.1 burnout fraction since it is progressively less attractive to use a large advanced engine. This is illustrated in figure 7(b) where the chemical-advanced hybrid results (the solid curve) are compared with the all-advanced results (the dashed line) for 3000 seconds specific impulse. The two curves are coincident from zero specific weight to 0.3, illustrating that the all-

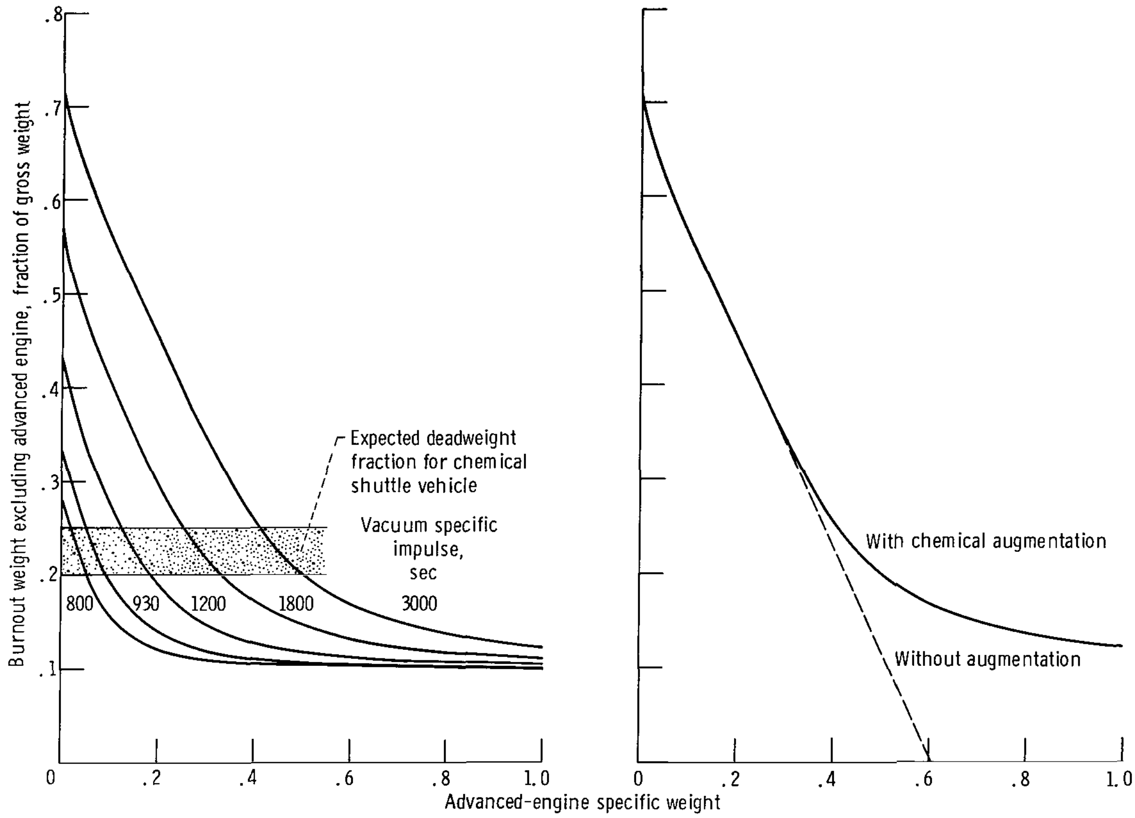

(a) Burnout weight fraction.

(b) Advantage gained by adding parallel-burn chemical boost phase to single-stage advanced-propulsion shuttle. Advanced-engine vacuum specific impulse, 3000 seconds.

Figure 7. - Performance of parallel-burn configuration (single-stage advanced-propulsion shuttle with chemical augmentation during boost phase). Final orbit, 83-kilometer-by-185-kilometer ellipse with 460-meter-per-second additional velocity increment ΔV capability.

advanced configuration is optimal when the advanced engine is light enough. For heavier advanced-engine weights, the performance of the parallel-boost hybrid flattens out, corresponding to the introduction of sizable amounts of chemical thrust. The 3000-second advanced engine is never "squeezed out" completely but (as will be shown) its optimal thrust level decreases toward 5 percent of initial gross weight as specific weight increases to 1.0.

Unfortunately, the parallel-burn boost technique yields improvements only for rather large advanced-engine specific weights, and the resulting weight fractions still tend to be marginal. Returning to figure 7(a), this may be seen by comparing the weight fraction shown against the band for the expected deadweight fraction of chemical shuttle stages. As before, a SCNR or dust-bed engine with 800 to 930 seconds specific impulse would need a specific weight lighter than 0.05 to merit consideration for this application. An 1800-second-specific-impulse engine still requires a specific weight less than 0.3 to look attractive.

Trajectory characteristics. - It can be seen in figure 8(a) that the addition of chemical augmentation can drastically alter the shape of the ascent trajectory. No alteration takes place, of course, for very lightweight advanced engines since chemical augmentation is then nonoptimal. In such cases, no chemical propulsion at all is used, and the optimum-thrust steering program begins at 30 kilometers. The curve shown in figure 8(a) for a specific engine weight of 0.5 shows the marked shift to lob-type trajectories when the advanced engine is relatively heavy. The peak altitude is 287 kilometers or about $3\frac{1}{2}$ times the burnout altitude (near perigee of the 83-km-by-185-km elliptic parking orbit). This is caused by the much smaller advanced-propulsion acceleration level for the sustainer phase. The amount of chemical augmentation is large in this case and leads to a much smaller advanced-propulsion thrust level than would otherwise be required. The propulsion transition altitude (chemical engine cutoff) is at 85 kilometers after 200 seconds of chemical-propulsion augmentation. The optimum-thrust trajectory portion also begins at this point.

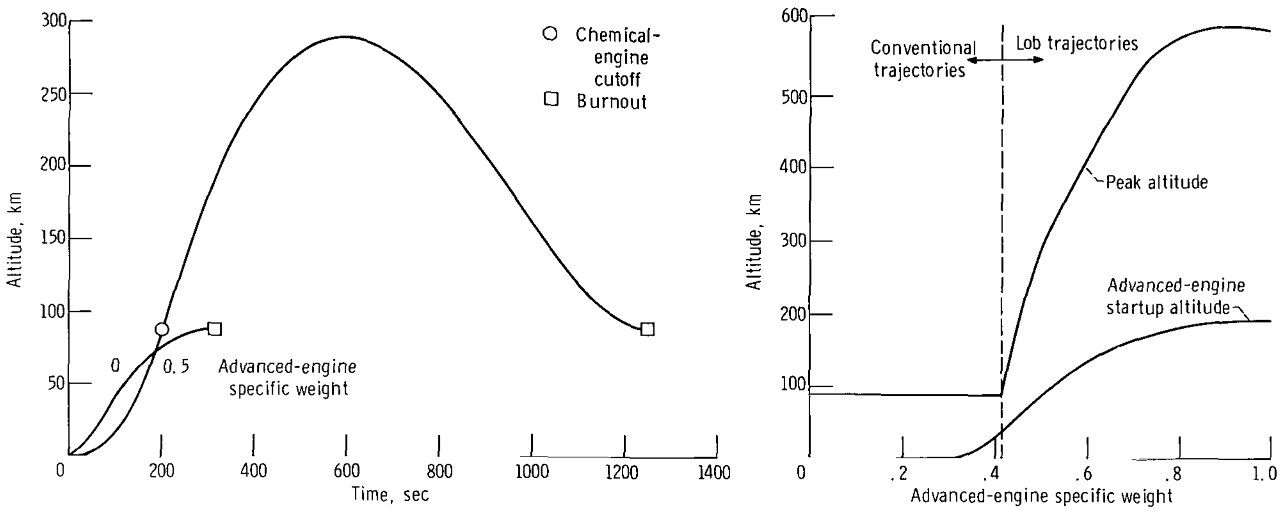

Figure 8. - Trajectory characteristics of parallel-burn configuration (single-stage advanced-propulsion shuttle with chemical augmentation during boost phase). Advanced-engine vacuum specific impulse, 3000 seconds; final orbit, 83-kilometer-by-185-kilometer ellipse with 460-meter-per-second additional velocity increment ΔV capability.

The variation of peak altitude and chemical-engine cutoff altitude with engine specific weight is given in figure 8(b) for the case of 3000 seconds specific impulse. There is a sharp kink in the peak altitude curve at a specific weight of 0.41 due to a change in the class of optimum trajectories. The two optimum trajectory classes are quite different and produce peak altitude curves that intersect each other rather than blending together smoothly. Conventional trajectories are best at specific weights below 0.41, and hence the peak and burnout altitudes are about the same. But at specific weights above 0.41 the lob-type trajectories are best because the sustainer phase is accomplished with relatively low thrust acceleration. This results in very high peak altitudes - as much as 600 kilometers for the heavier engines. The chemical-engine cutoff altitude curve shows that there is no benefit at all from using chemical augmentation unless the advanced-

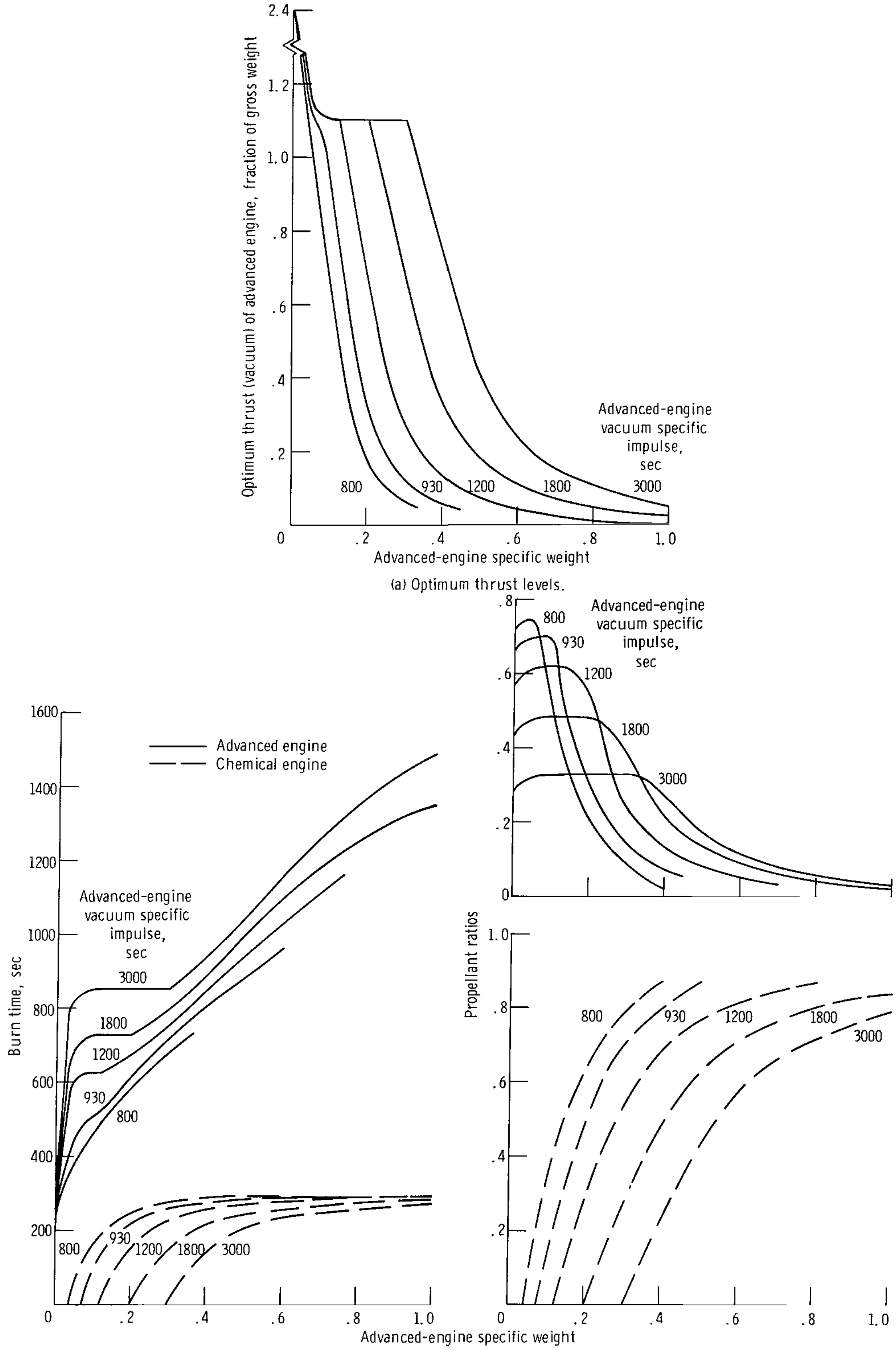

(a) Optimum thrust levels.

(b) Burn times.

(c) Propellant ratios.

Figure 9. - Design characteristics for parallel-burn configuration (single-stage advanced-propulsion shuttle with chemical augmentation during boost phase). Final orbit, 83-kilometer-by-185-kilometer ellipse with 460-meter-per-second additional velocity increment ΔV capability.

engine specific weight is greater than 0. 3. For heavier advanced engines the cutoff altitude increases rather steeply but levels off near 200 kilometers.

Design characteristics. - Figure 9 shows the thrust levels, propellant ratios, and engine burn times for the parallel-burn configuration. The dominant factor influencing all curves is the shift from all-advanced propulsion for lightweight engines to nearly all-chemical propulsion for heavyweight engines. At high specific engine weight, this leads to relatively small advanced-propulsion thrust levels, lower propellant ratios, and rather long burn times (as much as 25 min). The long burn times occur because the sharp drop in advanced-propulsion thrust level is accompanied by a relatively moderate drop in advanced propulsive effort. The odd shape of some curves is a result of two effects: First, at very small specific weight, the initial thrust-to-weight ratio rapidly decreases from 2. 4 to the limit value of 1. 2, and this produces flat spots in some curves between specific weights of 0. 05 and 0. 30. Secondly, there is a shift to lob-type trajectories after significant chemical augmentation is added, and this particularly affects the burn-time curves (creates discontinuities).

Single Hybrid Stage - Tandem-Burn Configuration (Chemical Burn Followed by Advanced Burn)

If an advanced-propulsion device is nonradioactive (e. g. , the beamed-energy rocket), the all-advanced-propulsion and parallel-burn hybrid configurations involve little safety hazard. However, for the more familiar nuclear devices, both of these configurations involve radiation hazards at low altitudes. These safety disadvantages are considerably lessened in the tandem burn configuration (fig. 1(c)) by delaying startup of the nuclear engine until the vehicle leaves the sensible atmosphere. Thus a 30-kilometer altitude constraint is applied to the transition from chemical to nuclear propulsion although the transition may occur at a greater altitude if this turns out to be optimum. In either case, the change to optimum-thrust steering coincides with the propulsion transition.

Performance. - In the high specific weight range, the performance of this configuration (fig. 10(a)) is essentially the same as for the parallel burn configuration - the nuclear engine is so heavy that it is best to practically eliminate it and retain only chemical propulsion. In the low specific weight range, the performance of the tandem-burn case is significantly worse than either of the other two single-stage cases. The decrease in burnout weight fraction at zero specific weight is between 21 and 37 percent depending on the specific impulse. Even for 2000 seconds specific impulse the specific weight must be less than 0. 1 to achieve attractive shuttle payloads.

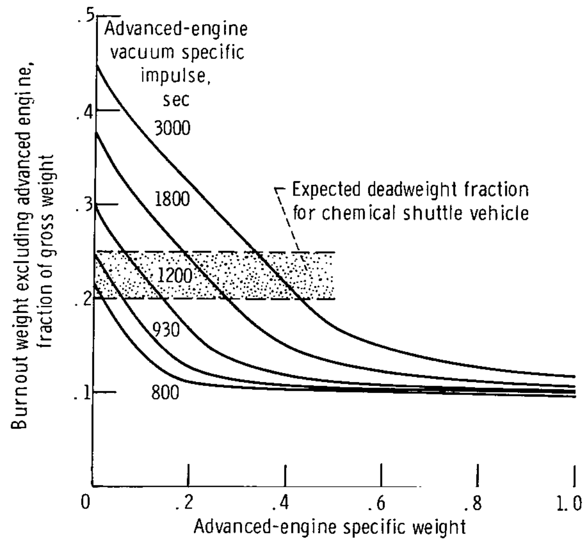

(a) Burnout weight fraction.

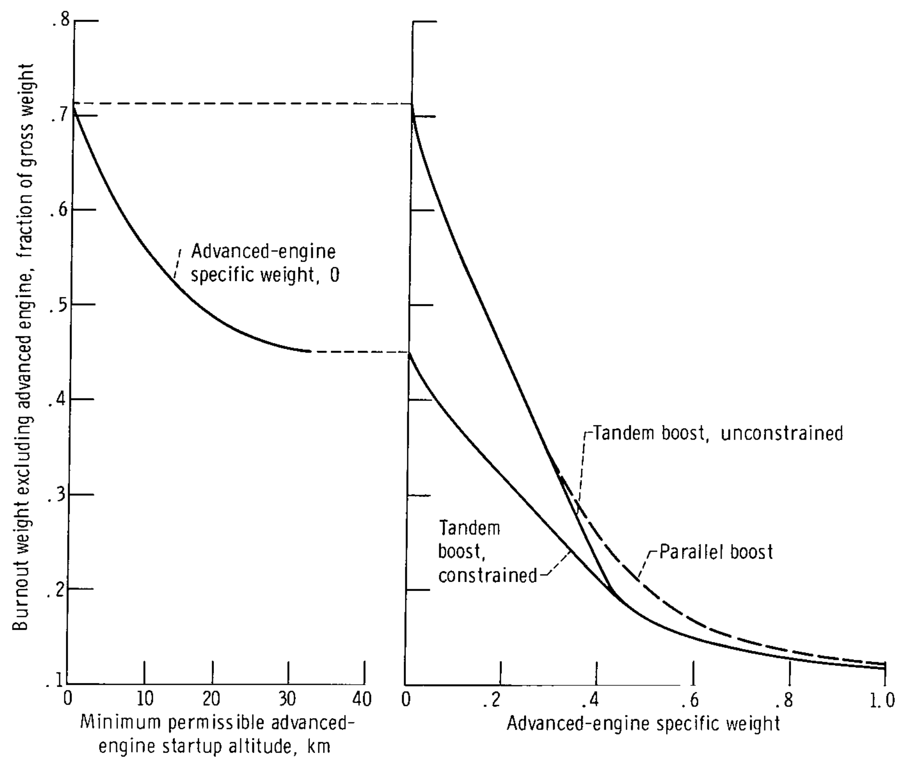

(b) Effect of advanced-engine startup altitude constraint. Advanced-engine vacuum specific impulse, 3000 seconds.

Figure 10. - Performance of single-stage shuttle tandem-burn configuration (chemical-propulsion boost phase followed by advanced-propulsion upper phase). Final orbit, 83-kilometer-by-185-kilometer ellipse with 460-meter-per-second additional velocity increment ΔV capability.

This performance penalty results from the restriction on nuclear engine startup altitude. The penalty could be decreased by lowering this limit. If the limit were removed entirely, the performance of this case would be no different from that of the all-nuclear case at low specific weight. This is illustrated in figure 10(b), which consists of two parts having the same ordinate but different abscissa scales. On the right, burnout weight fraction is plotted against nuclear engine specific weight for 3000 seconds specific impulse. The lower of the two solid curves gives the performance available with constrained (30 km) nuclear startup altitude; it is simply the topmost curve in figure 10(a). The upper solid curve shows the performance available from the tandem-boost shuttle when the constraint is removed. For lightweight engines (specific weight ≤ 0.3) this is identical to the previous all-nuclear or parallel-boost result; the chemical engine is "squeezed out" entirely. For heavy engines (specific weight ≥ 0.45), however, the results are identical with those shown previously in figure 10(a); the optimum transition altitude is already above the 30-kilometer limit. The advantage gained by using a parallel burning boost phase is indicated by the relatively small difference between the upper solid curve and the dashed curve. Thus, the comparatively large performance penalty that may be seen in comparing figures 10(a) and 7(a) may be attributed primarily to the effect of the nuclear engine startup altitude constraint.

The left portion of figure 10(b) shows the effect of reducing the constraint. Burnout weight fraction is plotted against minimum allowable nuclear startup altitude for 3000 seconds impulse and zero engine specific weight. As the horizontal dashed lines suggest, the left-hand curve may be considered to "interpolate" between the end points of the right-hand curves. Unfortunately, it does not appear that a small relaxation of the constraint will bring about any major performance gain. And eliminating or significantly reducing the constraint has the disadvantage of increasing the radiation hazard for many types of nuclear rockets. Hence, a significant performance-against-hazard tradeoff will be present in many cases.

Trajectory characteristics. - Figure 11 illustrates the trajectory characteristics of the tandem-burn case for 3000 seconds specific impulse. The trajectories are quite similar to those for the parallel-burn case and the same remarks made for them apply to these. Conventional trajectories are best at specific weights to 0.45, and the 30-kilometer altitude constraint is in effect. For heavier engines the lob-type trajectories are optimum, with peak altitudes to 600 kilometers and nuclear startup altitudes several times the constraint value.

Design characteristics. - The design characteristics for the tandem-burn case are shown in figure 12. These results are similar to those for the parallel-burn configuration, except for the effects caused by the 30-kilometer constraint on the nuclear startup altitude. For example, the constraint causes the chemical engines to burn at least 130 seconds and to consume at least 0.41 of the gross weight as fuel.

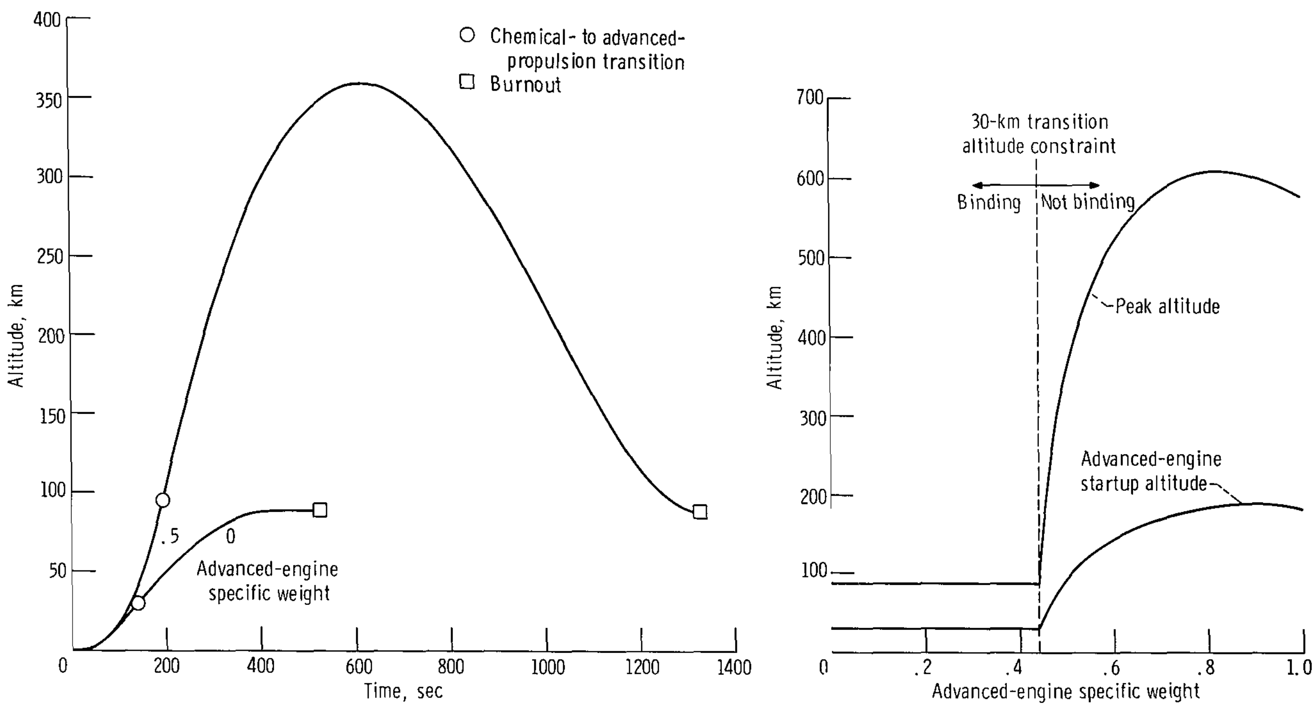

(a) Altitude-time histories.

(b) Peak altitude and propulsion transition altitude.

Figure 11. - Trajectory characteristics of a single-stage shuttle tandem-burn configuration (chemical-propulsion boost phase followed by advanced-propulsion upper phase). Advanced-engine vacuum specific impulse, 3000 seconds; final orbit, 83-kilometer-by-185-kilometer ellipse with 460-meter-per-second additional velocity increment ΔV capability.

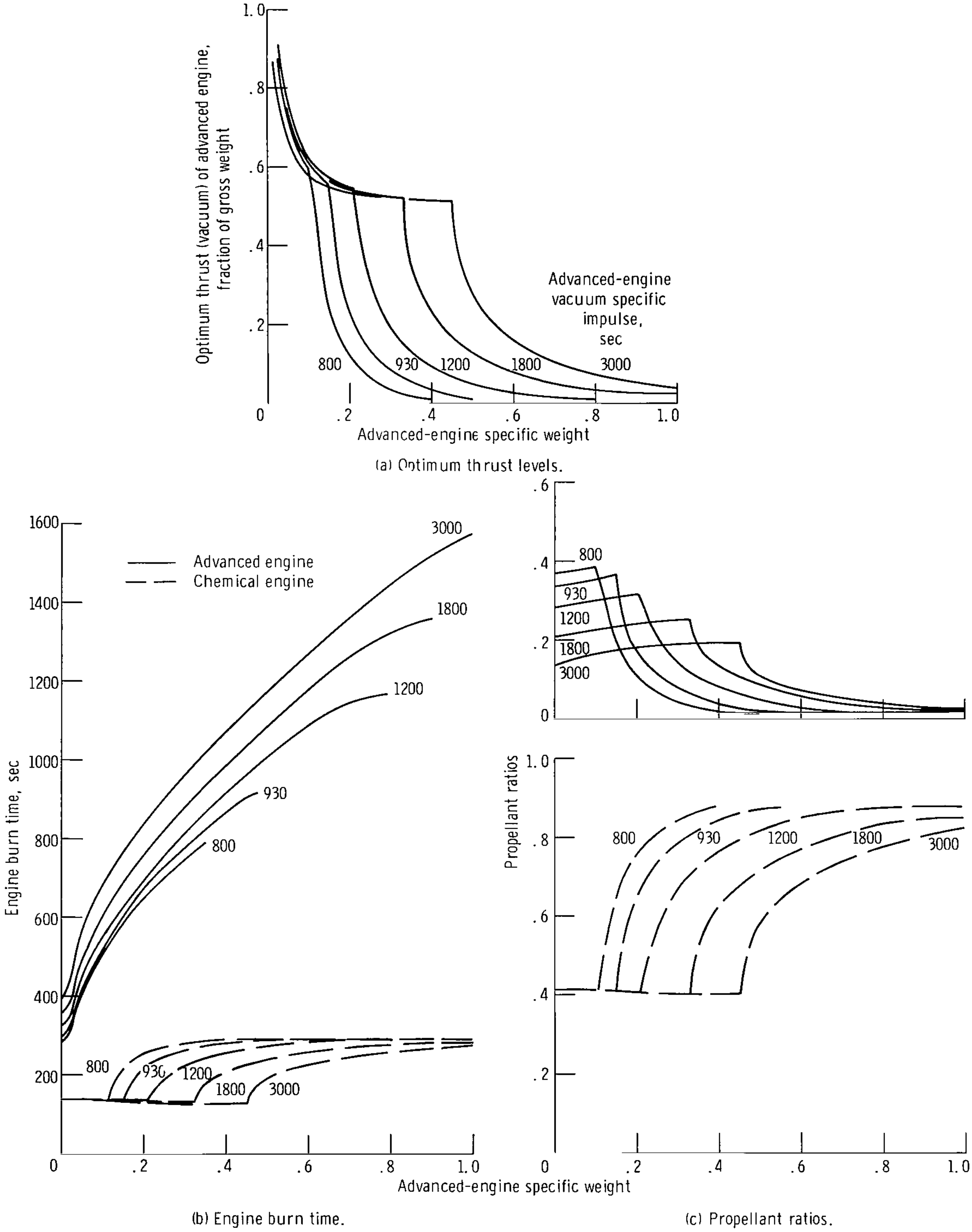

Figure 12. - Design characteristics for single-stage shuttle tandem-burn configuration (chemical-propulsion boost phase followed by advanced-propulsion upper phase). Final orbit, 83-kilometer-by-185-kilometer ellipse with 460-meter-per-second additional velocity increment ΔV capability.

Single-Stage Performance Comparison

The three single-stage configurations are compared on the basis of performance in figure 13 for 1800 seconds specific impulse. It is apparent that for anticipated deadweight fractions none of these configurations appears attractive unless the specific engine weight is less than 0.3. Between 0 and 0.2 specific weight the all-advanced-propulsion configuration delivers the most payload. If high-performance engines could actually be made at such low weights, an all-advanced-propulsion shuttle would yield truly spectacular performance. However, current designs fall far short of this goal.

At specific weights above 0.2, the parallel mode of chemical augmentation yields better performance than the all-advanced-propulsion mode, but the advantage is quite small in the region of expected deadweight fractions. The tandem mode of chemical augmentation with the 30-kilometer nuclear startup altitude constraint is unattractive unless specific weights less than 0.2 can be achieved.

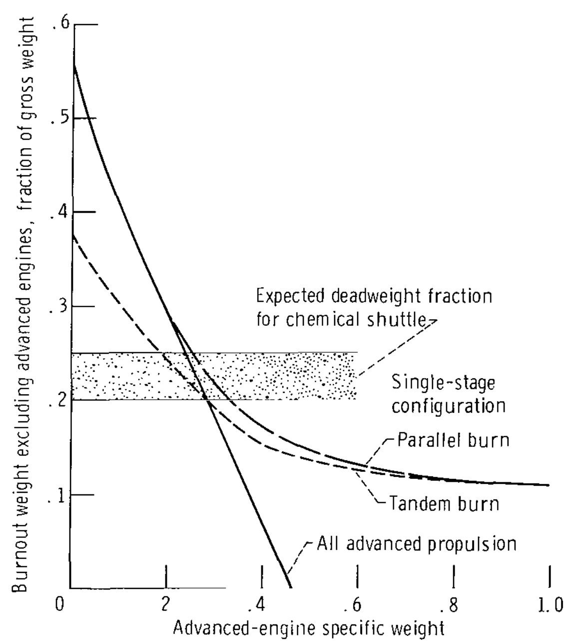

Figure 13. - Performance summary for single-stage shuttle Advanced-engine vacuum specific impulse, 1800 seconds; final orbit, 83-kilometer-by-185-kilometer ellipse with 460-meter-per-second additional velocity increment ΔV capability.

Two Stage - Chemical Booster Followed by Advanced Upper Stage

Recall that, for two-stage vehicles, it was necessary to assume definite values for $w_{ps,C}$ and $w_{ps,N}$, the first- and second-stage structure fractions, in order to locate an optimum staging point. As mentioned in the section ANALYSIS, values of 0.22 and 0.27, respectively, were assumed herein. These assumptions led to the results shown in figure 14(a), where the burnout weight fraction, this time also excluding the second-stage and jettisoned first-stage structure weights, is plotted as before against engine specific weight and impulse. The ordinates shown may be interpreted as consisting of payload plus any shielding and structure weight penalties due to the nuclear engine and its presumably less dense propellant.

These weight penalties do not apply to chemical stages, and in that case we obtain payload fractions in the neighborhood of 0.01 to 0.02, as indicated by the short line segment near the origin for 455 seconds specific impulse.

The more optimistic of the advanced engines clearly offer a potential for very substantial improvements, provided that the structure fractions of 0.22 and 0.27 can be

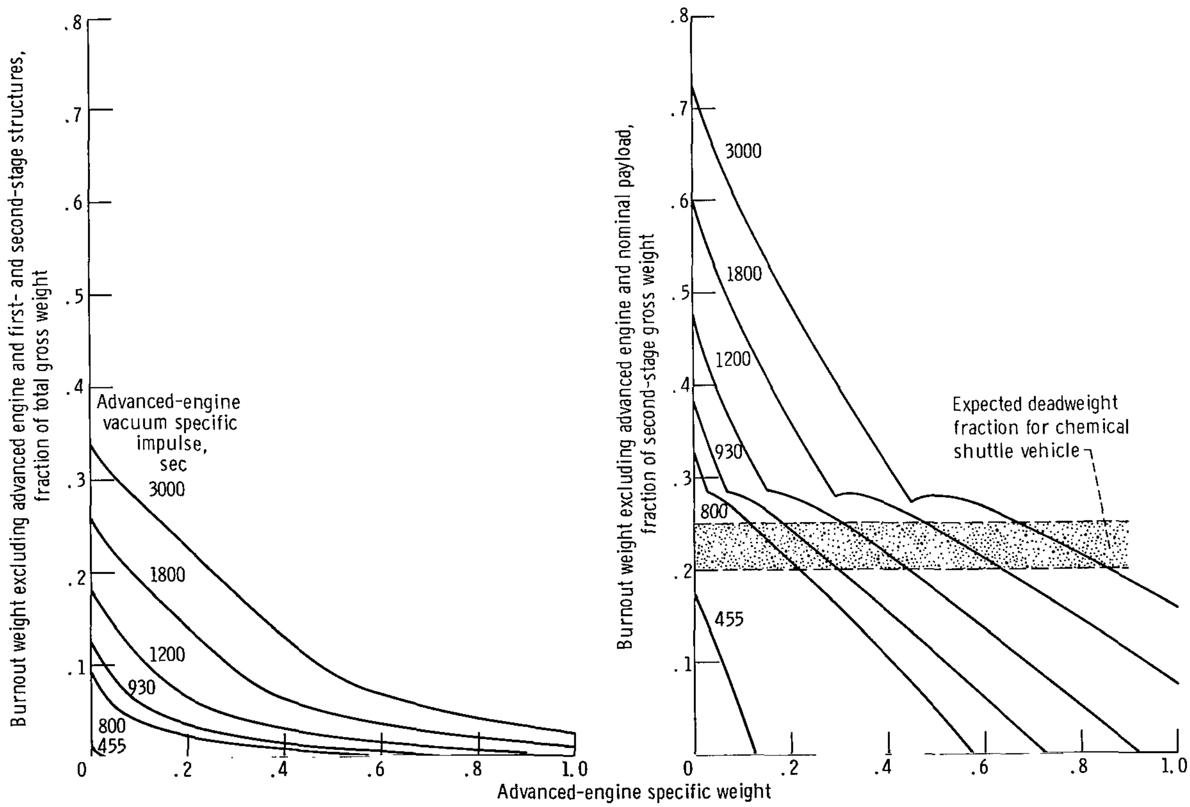

(a) Burnout weight fraction: chemical-stage fraction, 0.22; nuclear-stage structure fraction, 0.27.

(b) Upper-stage burnout weight fraction: chemical-stage structure fraction, 0.22; upper-stage structure fraction, 0.27. Nominal payload, 1.1 percent of gross ir'tial weight.

Figure 14. - Performance of two-stage shuttle with chemical booster stage and advanced-propulsion upper stage.

maintained. On the other hand, a $w_{ps, N}$ of 0.27 would appear decidedly optimistic for a recoverable upper stage employing nuclear engines and liquid hydrogen propellant. For example, if both the oxygen and hydrogen tanks of a presently envisioned shuttle stage were filled with pure liquid hydrogen, the apparent propellant-sensitive structure fraction w_{ps} would increase by a factor of 4 to 5. Radiation shielding would imply an additional penalty for manned vehicles. These penalties can be decreased (but probably not entirely offset) by reoptimizing the vehicle configuration, the structural design, and the staging point to account for the lower propellant density and the effects of engine-to-crew separation distance on shielding. Also helpful is the fact that propellant fractions are comparatively small for high-impulse systems; this implies that overall deadweight fractions (in terms of stage initial weight) would not increase drastically.

Figure 14(b) presents the second-stage burnout weight as a fraction of the second-stage initial weight. The entire first stage, the nuclear engine, and the nominal payload (1.1 percent of vehicle gross initial weight) are excluded, so that the ordinates shown represent the allowable structure plus shielding deadweight fractions (plus additional payload) for the second stage alone. These may be compared with the results of figures 4, 7(a), and 10(a) (after the same 1.1 percent nominal payload is deducted); and, like those, they are interpreted as a measure of design difficulty.

Typical altitude-against-time histories and the peak and staging altitudes are recorded in figures 15(a) and (b). In general, these are quite similar to those previously shown for the two single-stage, hybrid-propulsion cases. Lob-type trajectories are used for all but the lightest engines, and the 30-kilometer nuclear startup altitude con-

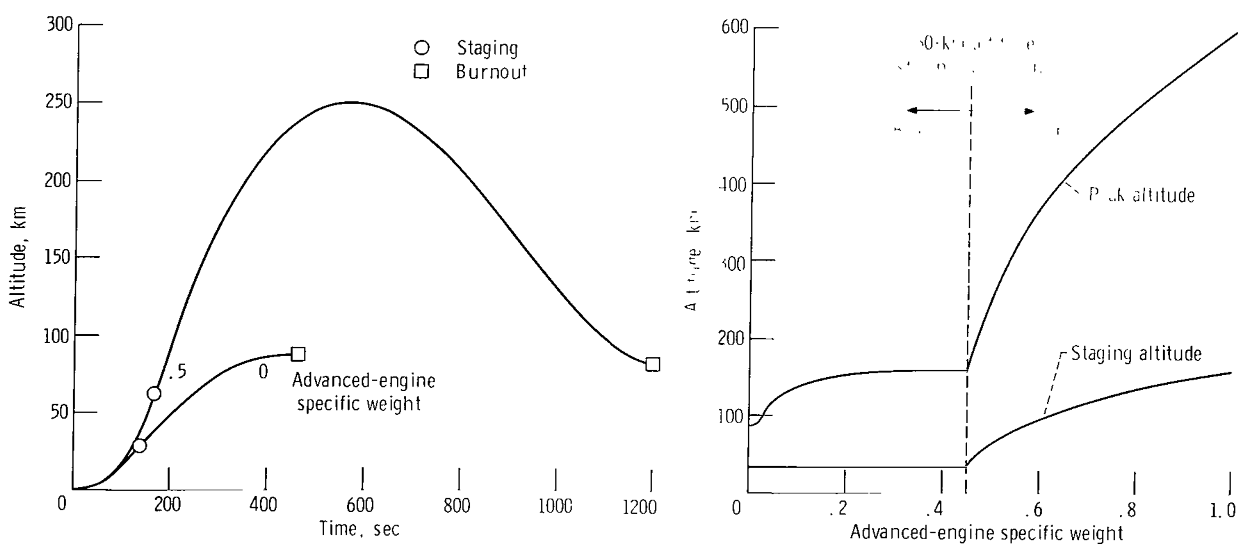

(a) Altitude-time histories

(b) Peak and staging altitudes.

Figure 15. - Trajectory characteristics of two-stage shuttle with chemical first stage and advanced-propulsion upper stage. Advanced-engine specific impulse, 3000 seconds

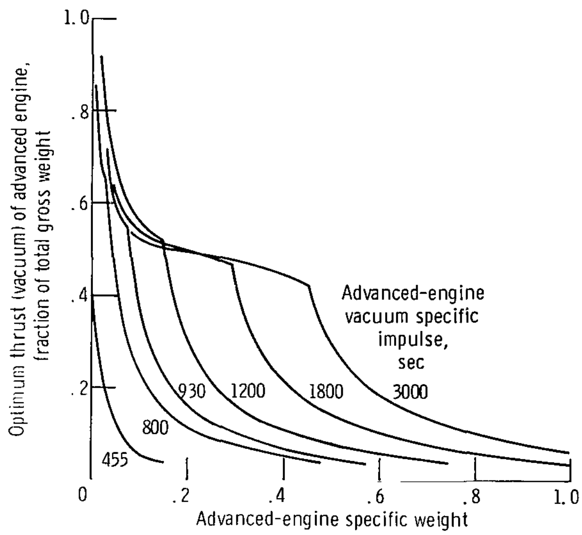

(a) Optimum thrust levels.

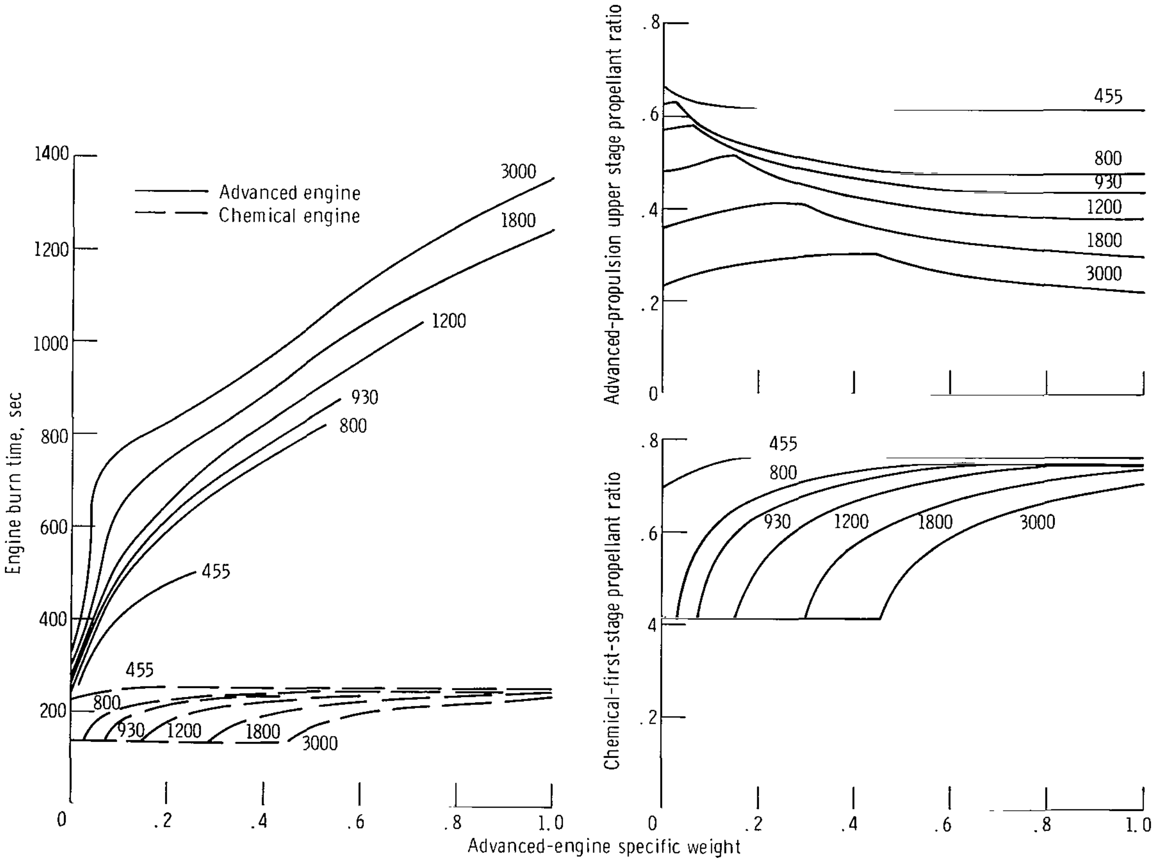

(b) Stage burn times.

(c) Propellant ratios.

Figure 16. - Design characteristics of two-stage shuttle with chemical first stage and advanced-propulsion upper stage.

straint is binding for engine specific weights less than about 0.45 (at 3000 sec specific impulse).

Figure 16(a) shows the optimum nuclear engine thrust levels obtained for the two-stage case. As in the hybrid cases, the "corner" clearly visible in each of these curves reflects the transition from constrained to unconstrained staging altitude trajectories as engine specific weight is increased. Stage burn times are shown in figure 16(b) and propellant ratios in figure 16(c). It should be appreciated that the vehicle design parameters illustrated in figure 16 are relatively sensitive to deviation from the assumed structural weight fraction; that is, a small change from the baseline values (0.22 and 0.27 for first and second stages, respectively) may result in a major shift in the optimal staging point. This would imply large changes in stage masses, propellant fractions, engine sizes, burn times, and trajectory shaping. However, the consequent change in payload after reoptimization of these factors would be fairly small.

CONCLUDING REMARKS

A parametric survey of earth-to-low-orbit launch trajectories has been presented herein. These results apply to hypothetical advanced engines with 800 to 3000 seconds specific impulse and engine-weight-to-thrust ratios from 0 to 1.0. Four representative vehicle-trajectory combinations were considered: single-stage vehicles with either (1) a single advanced engine, (2) an initial parallel chemical- and advanced-propulsion phase followed by an advanced-propulsion phase (parallel burn), or (3) a chemical boost phase followed by an advanced-propulsion sustainer phase (tandem burn); and (4) a two-stage vehicle, chemical-engine booster stage and advanced-engine upper stage.

These results are intended primarily as an aid in evaluating advanced propulsion concepts from the earth-to-low-orbit launch mission viewpoint. Near-optimum design data (e.g., stage propellant loadings, engine sizes, and burn times) from the present results may be used as inputs for preliminary vehicle-structure, shielding, and engine system analyses. The resultant deadweight fraction may then be combined with the present results to evaluate performance and feasibility. Alternatively, structural deadweights from previous (e.g., chemical shuttle stage) analyses may be interpreted as lower bounds for functionally similar stages employing advanced engines and pure liquid hydrogen propellant.

In general, it was found that major performance penalties resulted when ground start was replaced by a high-altitude start at 30 kilometers or above. The high-altitude start, however, is clearly desirable from the standpoints of environmental contamination, radiation hazard, and shielding if the advanced engine is a nuclear fission device. In this case it appears that a two-stage vehicle configuration will be needed.

Further study is recommended to better define the structural characteristics and radiation shielding requirements of earth-to-orbit launch stages employing advanced propulsion concepts. It should be clearly appreciated that the associated structure and shielding requirements have a major effect on the apparent usefulness of a future engine concept. Many advanced high-thrust engine concepts require liquid hydrogen for propellant. In this case, because of the low bulk density compared to conventional fuels such as a combination of oxygen and hydrogen, it will be very difficult and perhaps impossible to maintain the present structural deadweight fraction in a single-stage airplane-like vehicle. In that case it might be necessary to abandon the "fly-back" recovery concept (relying instead on recovery at sea) in order to achieve structures light enough for a single-stage, advanced-engine shuttle vehicle.

Lewis Research Center,
National Aeronautics and Space Administration,
Cleveland, Ohio, February 8, 1972,
110-06.

REFERENCES

1. Meghreblian, Robert V.: Gaseous Fission Reactors for Booster Propulsion. Tech. Rep. 32-94, Jet Propulsion Lab., California Inst. Tech., Mar. 31, 1961. (Also ARS J., vol. 32, no. 1, Jan. 1962, pp. 13-21.)
2. McGolrick, J. E.; and Davis, B. W.: Launch Vehicles for Future Automated Space Missions. J. Spacecraft Rockets, vol. 6, no. 2, Feb. 1969, pp. 129-135.
3. Salkeld, Robert: Deep Space Shuttles: Chemical vs Nuclear; Direct Flight vs Near-Orbit Rendezvous. J. Spacecraft Rockets, vol. 7, no. 11, Nov. 1970, pp. 1369-1371.
4. Clark, M. Ray; Sagerman, Gary D.; and Lahti, Gerald P.: Comparison of Small Water-Graphite Nuclear Rocket Stages with Chemical Upper Stages for Unmanned Missions. NASA TN D-4827, 1968.
5. Cooper, Ralph S.: Advanced Nuclear Propulsion Concepts. Paper 65-531, AIAA, July 1965.
6. Ragsdale, Robert G.: Some Fuel Loss Rate and Weight Estimates of an Open-Cycle Gas-Core Nuclear Rocket Engine. Paper 70-690, AIAA, June 1970.

7. Ragsdale, Robert G.: Relationship Between Engine Parameters and the Fuel Mass Contained in an Open-Cycle Gas-Core Reactor. Research on Uranium Plasmas and their Technological Applications. NASA SP-236, 1971, pp. 13-22.

8. Fishbach, Laurence H.: Mission Performance Potential of Regeneratively Cooled Gas-Core Nuclear Rockets. NASA TM X-2256, 1971.

9. McLafferty, G. H.; and Bauer, H. E.: Studies of Specific Nuclear Light Bulb and Open-Cycle Vortex-Stabilized Gaseous Nuclear Rocket Engines. NASA CR-1030, 1968.

10. Rom, Frank E.; and Putre, Henry A.: Laser Propulsion. NASA TM X-2510, 1972.

11. Spurlock, Omer F.; and Teren, Fred: A Trajectory Code for Maximizing the Payload of Multistage Launch Vehicles. NASA TN D-4729, 1968.

NASA-Langley, 1972 —— 31 E-6749

NATIONAL AERONAUTICS AND SPACE ADMISTRATION
WASHINGTON, D.C. 20546

OFFICIAL BUSINESS
PENALTY FOR PRIVATE USE $300

FIRST CLASS MAIL

POSTAGE AND FEES PAID
NATIONAL AERONAUTICS AND
SPACE ADMINISTRATION

U.S.MAIL

018 001 C1 U 31 720414 S00903DS
DEPT OF THE AIR FORCE
AF WEAPONS LAB (AFSC)
TECH LIBRARY/WLOL/
ATTN: E LOU BOWMAN, CHIEF
KIRTLAND AFB NM 87117

POSTMASTER: If Undeliverable (Section 158 Postal Manual) Do Not Return

---

"The aeronautical and space activities of the United States shall be conducted so as to contribute . . . to the expansion of human knowledge of phenomena in the atmosphere and space. The Administration shall provide for the widest practicable and appropriate dissemination of information concerning its activities and the results thereof."

—NATIONAL AERONAUTICS AND SPACE ACT OF 1958

NASA SCIENTIFIC AND TECHNICAL PUBLICATIONS

TECHNICAL REPORTS: Scientific and technical information considered important, complete, and a lasting contribution to existing knowledge.

TECHNICAL NOTES: Information less broad in scope but nevertheless of importance as a contribution to existing knowledge.

TECHNICAL MEMORANDUMS: Information receiving limited distribution because of preliminary data, security classification, or other reasons.

CONTRACTOR REPORTS: Scientific and technical information generated under a NASA contract or grant and considered an important contribution to existing knowledge.

TECHNICAL TRANSLATIONS: Information published in a foreign language considered to merit NASA distribution in English.

SPECIAL PUBLICATIONS: Information derived from or of value to NASA activities. Publications include conference proceedings, monographs, data compilations, handbooks, sourcebooks, and special bibliographies.

TECHNOLOGY UTILIZATION PUBLICATIONS: Information on technology used by NASA that may be of particular interest in commercial and other non-aerospace applications. Publications include Tech Briefs, Technology Utilization Reports and Technology Surveys.

Details on the availability of these publications may be obtained from:

SCIENTIFIC AND TECHNICAL INFORMATION OFFICE

NATIONAL AERONAUTICS AND SPACE ADMINISTRATION

Washington, D.C. 20546